

A comparative study between 4 optimal DWI gradient sampling schemes: simulations based on constrained spherical deconvolution (CSD)

S-P. Lee¹, J-D. Tournier², C-P. Hess³, C-M. Chen¹, and W-Y. I. Tseng⁴

¹Institute of Biomedical Engineering, National Taiwan University, Taipei, Taipei, Taiwan, ²Brain Research Institute, Florey Neuroscience Institutes, Austin, Melbourne, Australia, ³Department of Radiology, University of California-San Francisco, San Francisco, California, United States, ⁴Center for Optoelectronic Biomedicine, National Taiwan University Medical College, Taipei, Taiwan

Introduction:

The constrained spherical deconvolution (CSD) approach has been shown to be robust to resolve fibers crossing at small angles [1]. Nevertheless, the DW gradient sampling scheme is also crucial to obtain an accurate reconstruction of the fiber orientation distribution (FOD), although the optimal scheme to use with high angular resolution DW imaging (HARDI) methods has not been fully investigated. The goal of this study is to determine the optimal sampling scheme for use with CSD, in terms of the precision of the estimated fiber orientations. This will improve the reliability of performing white matter tractography through crossing fiber regions.

Material & Methods:

Simulated data sets were generated along 60 DW directions assuming two b -value (1000 and 3000 s/mm^2) and a model consisting of two tensors (FA = 0.8) with equal volume fractions, crossing two group at 3 different angles, (35°, 40° and 45°) and (30°, 35° and 40°), respectively. Rician noise with SNR = 20 was added to the signal intensities and 100 trials were performed for each set of parameters. The CSD algorithm was used to compute the FOD obtained using super-CSD with $l_{max}=16$. Furthermore, each FOD exhibited that the opaque surface corresponds to the mean FOD over 100 tests whereas the transparent surface corresponds to the mean + 2 standard deviations.

We compared 4 DW gradient sampling schemes, generated using the following methods: modified electrostatic repulsion (modified Jones 60) [2], electrostatic repulsion (Jones 60) [2], recursive zonal area equal area sphere partitioning (EQ) [3], and generalized spiral sets [4]. Each method generates a non-symmetric sampling scheme with 60 non-collinear directions. The repulsion term was set to r^{-2} for the Jones 60 scheme, and to r^{-128} for the modified Jones 60 scheme. The spiral sets consists of points on the curve traced by a ship traveling from one pole to the other at a fixed angle. EQ partition is a partition of S^2 into a finite number of regions of equal area. The area of each region is defined using the Lebesgue measure inherited from R^3 .

Three statistical parameters were used to evaluate performance: success rate, angular error, and volume ratio. The success rate was defined as the percentage of trials where the two fiber orientations can be resolved, each with amplitude over 0.2. The angular error was defined as the average orientation error between the estimated and true fiber orientations. The volume ratio was defined as the ratio of the second largest peak intensity to the maximum peak intensity.

Results:

All sampling schemes performed well, and provided broadly similar results. Overall, the modified Jones 60 method provides slightly higher precision than the other 3 sampling schemes, and produces clearer separation between the fiber orientations in the FODs (Fig. 1 and 2). It also has a generally higher success rate, small angular error and large volume ratio (Table 1 and 2).

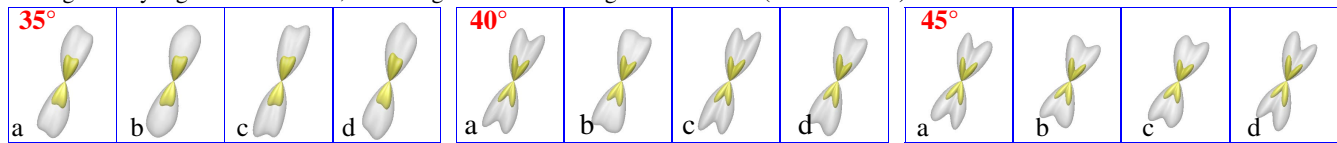


Fig 1: FODs obtained from $b = 1000 s/mm^2$ using CSD at the 3 crossing angles: 35° (left), 40° (middle), and 45° (right). For each crossing angle, the FOD obtained using each gradient sampling scheme is shown: (a) modified Jones 60, (b) Jones 60, (c) EQ partition, (d) spiral sets.

schemes	modified Jones 60	Jones 60	EQ partition	spiral sets	schemes	modified Jones 60	Jones 60	EQ partition	spiral sets	schemes	modified Jones 60	Jones 60	EQ partition	spiral sets
35°					40°					45°				
Angular error	6.88°	7.32°	7.21°	7.22°	Angular error	6.73°	7.36°	7.14°	7.42°	Angular error	7.11°	6.98°	7.55°	7.15°
mean (std)	(4.06°)	(4.58°)	(3.80°)	(4.57°)	mean (std)	(4.21°)	(4.67°)	(4.10°)	(4.63°)	mean (std)	(3.18°)	(3.94°)	(3.57°)	(3.74°)
Volume ratio	62.01%	62.39%	59.24%	64.58%	Volume ratio	66.83%	69.47%	64.54%	66.71%	Volume ratio	74.36%	77.49%	72.24%	73.69%
mean (std)	(23.06%)	(22.94%)	(22.23%)	(21.83%)	mean (std)	(18.09%)	(19.47%)	(18.32%)	(20.50%)	mean (std)	(15.07%)	(14.92%)	(16.29%)	(15.80%)
Success rate	83%	84%	85%	85%	Success rate	100%	98%	100%	98%	Success rate	100%	99%	100%	100%

Table 1: statistical parameters obtained at the 3 crossing angles: 35° (left), 40° (middle), and 45° (right). For each crossing angle, the statistics obtained using each gradient sampling scheme are shown.

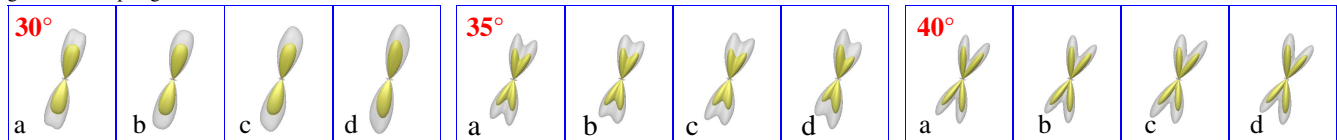


Fig 2: FODs obtained from $b = 3000 s/mm^2$ using CSD at the 3 crossing angles: 30° (left), 35° (middle), and 40° (right). For each crossing angle, the FOD obtained using each gradient sampling scheme is shown: (a) modified Jones 60, (b) Jones 60, (c) EQ partition, (d) spiral sets.

schemes	modified Jones 60	Jones 60	EQ partition	spiral sets	schemes	modified Jones 60	Jones 60	EQ partition	spiral sets	schemes	modified Jones 60	Jones 60	EQ partition	spiral sets
30°					35°					40°				
Angular error	5.71°	6.02°	5.22°	6.29°	Angular error	4.32°	4.04°	4.32°	4.79°	Angular error	3.25°	3.40°	3.70°	3.44°
mean (std)	(3.38°)	(3.84°)	(3.52°)	(3.58°)	mean (std)	(2.45°)	(1.93°)	(2.39°)	(2.77°)	mean (std)	(1.30°)	(2.19°)	(2.27°)	(1.72°)
Volume ratio	72.52%	72.98%	73.67%	71.10%	Volume ratio	80.49%	79.01%	75.48%	77.33%	Volume ratio	86.16%	87.51%	82.01%	84.63%
mean (std)	(21.10%)	(21.86%)	(21.29%)	(22.16%)	mean (std)	(13.53%)	(13.68%)	(16.71%)	(16.28%)	mean (std)	(8.92%)	(8.43%)	(12.81%)	(9.98%)
Success rate	39%	36%	36%	41%	Success rate	96%	87%	94%	89%	Success rate	100%	99%	100%	100%

Table 2: statistical parameters obtained at the 3 crossing angles: 30° (left), 35° (middle), and 40° (right). For each crossing angle, the statistics obtained using each gradient sampling scheme are shown.

Conclusion

While all four sampling schemes provide near-equivalent performance, the modified Jones 60 scheme seems slightly superior to the other sampling schemes across b -values and crossing angles. While in the $b = 1000 s/mm^2$ with 35° crossing angle case, modified Jones 60 has generally lower success rate than the others, it still has a generally smallest angular error. As crossing angle becomes larger, modified Jones 60 provides a generally higher success rate and more accurate gradient directions (Tables 1 and 2). However, the results show that any of these four schemes can be used with very similar results.

References

[1] Tournier *et al.*, NeuroImage 42: 617-625 (2008). [2] Jones et al., MRM 42: 515-525 (1999). [3] Paul Leopardi et al., ETNA 25: 309-327 (2006). [4] E. B. Saff and A. B. J. Kuijlaars., Mathematical Intelligencer 19: 5-11 (1997).